Propagation Loss Model for Neighborhood Area Networks in Smart Grids

Muhammad Babar Ali, Wolfgang Endemann, and Rüdiger Kays

***Abstract*—Currently the power sector is striving for the efficient utilization of its generation capabilities in existing distributed energy networks. In future smart grids, applications like automated meter reading, direct load control with demand side management, and charging points for electric vehicles in multistory parking plazas will pose a strong communication challenge to the RF planners. One of the main objectives is to design a realistic link budget for outdoor-to-deep-indoor wireless communication scenarios while utilizing the existing grid infrastructure. This paper presents a realistic two-slope empirical path loss model to predict power requirements for the wireless link between smart meters in prosumer premises and remote utility/grid devices presumably available in near vicinity. The proposed model is based on measurements performed over three sub-gigahertz frequency bands (200 MHz, 434 MHz, and 868 MHz) and the 2.4 GHz band. It supports outside, inside and in-basement deployment of the smart meter communication unit.**

***Index Terms*—Propagation loss model, smart grid communications, smart metering, wireless channel model, wireless sensor networks.**

I. Introduction

WIRELESS communication is the key to realize future smart power grids, and it is the best option for retrofitting existing smart grids (SG) as an efficient approach towards economic solutions. As a critical infrastructure, smart grid operations highly depend on reliable wireless links. Its radio attributes must satisfy the minimum requirements for successful communication. However, the potential to improve network reliability in wireless communication is limited by the available resources. These resources are bounded either by fundamentals of physics or by the regulatory authorities. These restrictions mainly apply to frequency band, bandwidth, transmit power, channel access modes and their usage. A successful network design depends on the suitability of the selected communication technology and the band. Critical use cases must carefully consider channel characteristics, such as multipath fading and propagation losses. Best planning decisions to adopt a certain technology and its deployment demand precise knowledge on ground realities of these characteristics. Propagation models for inside-to-outside communication (I2O) usually reflect the penetration losses of a single outer wall. In many use cases of SG ecosystems, transceivers may be located at nearly the center of subterranean floors of buildings. In literature, these links are formally categorized as deep indoor links [1]. Such wireless links experience excess attenuation. This attenuation arises from both the horizontal depth from the outermost wall and vertical depth from the ground level. An enlarged path loss exponent often models this attenuation. This paper proposes a path loss model with the focus on penetration loss.

Today, energy systems operate on high stability with rare blackouts since there exist a central control and highly intelligent mechanisms to balance electric power. European vision is to produce not less than 80% of its energy from renewable sources by 2050 [2], moving towards climate neutral economy [3]. Therefore, energy utilities are digging deep into multiple strategies. These strategies target on centralized automation of energy consumption in commercial and residential buildings. Utilities are currently practicing as well as promoting integration of distributed energy resources (DER) at distribution and prosumer level [4]. The dense penetration of non-inertial DERs such as photovoltaic (PV) cells will provoke power system instabilities in secondary distribution networks [5]. Therefore, they require frequent monitoring and control. Options to serve this challenge may include improvements in power electronics, hierarchical distributed control models [6] and islanded operation to support nanogrid/virtual power plants (VPP) [7]–[9].

Though this paper focusses on wireless communication, we want to point out that in order to deploy SG neighborhood area network (NAN), preference might be given to power line communication (PLC) over wireless communication for backhaul at smaller distances [10] or delay-tolerant applications [11]. A hybrid of PLC and wireless communication are also feasible [12]. Wireless technologies such as IEEE 802.15.4, IEEE 802.11, Long Term Evolution (LTE) 5G and LTE 450 operate in various frequency bands (2.4 GHz, 5 GHz, 1800 MHz, and sub-1 GHz bands). An appropriate wireless technology in an industrial, scientific and medical (ISM) band also curtail the incurred cost for frequency resource. The wireless NAN with smart meter communication units (SMCU) and distribution transformers (DT) locations can play a key role to bring smart grid vision into reality [8]. In current SG NANs, in urban and suburban areas, SMCUs are often installed inside subterranean rooms of residential or commercial buildings. On the other hand, DTs are approximately 2–3 m high above ground where utility uses underground laterals. These readily available DT locations can be used to install communication devices such as data collectors (DC). DCs can forward data to a control center. These SMCUs and pad mounted DTs neither

Manuscript received September 10, 2021; revised April 6, 2022; approved for publication by Davy Gaillot, Division II Editor, April 18, 2022.

The authors are with the Communication Technology Institute at TU Dortmund University, 44227 Dortmund, Germany, email: {babar.ali, wolfgang.endemann, ruediger.kays}@tu-dortmund.de. See http://www.kt.e-technik.tu-dortmund.de/.

M. B. Ali is the corresponding author.

Digital Object Identifier: 10.23919/JCN.2022.000017

1229-2370/22/$10.00 © 2022 KICS

provide suitable antenna height nor favor directional antennas due to inside-to-outside characteristics of SMCU-DC wireless links. Furthermore, in current European grid infrastructures, the distance between the SMCU and the nearest DC is about 500 m or less. Therefore, it is important to design a reliable SMCU-DC link with fair comparison of various frequency bands, for the hierarchical control of RES.

SMCU-DC link budget estimation might utilize existing channel models from the literature for candidate frequencies. These estimations predict the link budget; however, the utilized models might use different measurement situations and methodologies. Therefore, these estimations cannot provide reasonable link budgets for the fair comparison of propagation losses over different frequency bands. Furthermore, SMCU-DC links, with SMCUs in a basement, also require accurate penetration loss assessments derived from similar situations and methodologies. The propagation models might also become unreliable when received signal strength indicator (RSSI) samples from commercial off-the-shelf wireless modules are used as these measurements are subject to produce module-specific results [13] as well as errors due to extrinsic and intrinsic factors [14]. The authors therefore derived the proposed path loss model for 200 MHz, 434 MHz, 868 MHz, and 2.4 GHz, from measurements:

- Over the set of frequency bands of interest
- In all situations of interest
- Solely based on measurements performed by the authors
- Using the same methodology
- Using the same equipment
- At the same set of locations for all frequencies

These measurements are stringent and more reliable in contrast to a meta-study. Therefore, this paper presents these measurements and uses these to derive a proposal for modeling wireless channels for smart grids in suburban environments. To the best of the authors' knowledge, there is no publication to predict propagation losses in SG NANs with frequencies of 200 MHz up to 2.4 GHz for this specific application scenario (up to 500 m distance, transceiver antenna height of about 1 m and attenuation due to underground position of transmitters).

This paper structure is as follows: Section II discusses existing channel models. Section III describes the measurement campaigns, followed by the key results in Section IV. We propose and discuss our path loss model in Section V and give a conclusion in Section VI.

II. Existing Channel Models

Deep indoor communication is a challenge for RF planners in traditional cellular networks and also in smart grid ecosystems. In literature, an extensive work is available for path loss (PL) estimations in indoor as well as outdoor mobile communication environments. For the basic wireless transmission losses for linearly polarized transceivers and free space path loss model, we refer to Harald. T. Friis' free space model. The authors of [15], [16] discussed empirical path loss models such as Hata-Okumura model and COST231-Hata. A comparative analysis of 30 path loss models, developed from 1999 to 2007 is presented in [17]. Table I summarizes the PL models discussed in this section.

TABLE I
PATH LOSS MODELS.

Band (MHz)	d_0 (m)	$L(d_0)$ (dB)	$\eta(\sigma)$ - (dB)	Environment	Ref.
169	10	102	-1.3 (15.1)	I2O: SU	[18]
434	10	106	-1 (10.9)	I2O: SU	
868	10	111	-0.6 (10.0)	I2O: SU	
2400	1	40.33	2.58 (3.06)	O2O: SS	[14]
868	1	26.81	3.1 (3.56)	Indoor: Home	[19]
2400	1	27.75	4.2 (5.94)	Indoor: Home	
879	1	31.8	2.7	O2O: U	[20]
800	1k	138.47	4.31	O2O: SU-P	[21]
800	1k	125.67	3.46	O2O: SU-TT	
868	1k	140.7	3.12 (9.7)	O2O: SU	[22]
2400	1	40.14	1.72 (2.18)	O2O: SS-VNA	[13]
2400	1	63.28	1.99 (1.07)	O2O: SS-MicaZ	
2400	1	56.82	1.64 (1.86)	O2O: SS-Iris	

* $L(d_0)$=Path Loss at distance d_0, SU=Suburban, U=Urban, SS=Substation, TT=Tree Track, P=Park

A. Propagation Loss for Indoor Communication

This section discusses various propagation loss models, which consider building penetration losses over wireless link between outdoor and indoor device.

The authors in [23] evaluated signal attenuation in a deep indoor environment. In their experiment, they used custom-built transceivers. They installed software defined radio receivers on the roof of a multistory building and randomly spread 50 transmitters inside the building on various floors. From the results collected at the receivers, they perceived normally distributed signal attenuations with a mean value of 33.7 dB, 31.8 dB and 39.6 dB at 169 MHz, 434 MHz, and 868 MHz, respectively. This value can simply be added to the free space path loss model as a crude estimation. They also claimed that the frequency selective fading is more prominent in 868 MHz due to higher bandwidth of its channels as compared to narrow bandwidth of 169 MHz and 434 MHz ranges. In [24], the authors presented RSSI based measurement statistics to highlight the distant patterns in propagation losses in indoor environment (basements and ground level). These measurements reflected that narrow band internet of things (NB-IoT) signals, transmitted from an operator's tower at 820.5 MHz, requires 13 dB more power to reach inside basements than to reach inside ground floor. They also found that the outdoor to indoor (O2I) 3GPP model [25] fits well to these measurements on ground. However, it cannot predict the signal drop at every point on a floor below ground at level -1 or -2.

Noticeable contradictions as well as variations in building penetration losses (BPL) are pointed out by Fuschini *et al.* [26]. Furthermore, they measured BPL in the European smart metering environment and observed the BPL of 7.5 dB with $\sigma = 4.5$ dB standard deviation at 169 MHz band. However, a comparison with potential frequency bands using

(a) Receiver locations when the transmitter is in sanitation room of the basement (TxSite: 'basement-0').

(b) Receiver locations when the transmitter is inside the building (TxSite: 'InHouse'), or outside the building (TxSite: 'Outside').

Fig. 1. Exact locations of the receiver up to ≈15 m, outside ET Building (TxSites: InHouse, Outside and basement-0).

similar hardware needs further attention. An average building entry loss (BEL) of 61 dB at 1.5 GHz is reported in [27] from the sides of the office building. At 3 GHz, this BEL is 10 dB higher than that of 1.5 GHz. The BEL of 11 dB to 27 dB is reported in [28] for various sections of the building at 3 GHz. The author [29] presented propagation losses in multistory buildings at 900 MHz while Kacou *et al.* [19] presented a multiwall path loss model for 800 MHz to 6 GHz in a residential single story building.

B. Propagation Loss for Outdoor Links

With limited literature in path loss modelling for center frequencies<500 MHz, the article [30] seems to be the recent one which estimated LTE channel characteristics at 463 MHz. The authors executed a measurement campaign in suburban areas to collect reference signal receive power (RSRP). They suggested a new model based on the Hata model. The proposed model is also within the limits of Winner Suburban Macro models. However, authors never rated its supremacy for wireless transmission over other potential sub-GHz bands. RSSI based field measurements are presented in [14]. First, the authors comprehensively discuss intrinsic and extrinsic imprecision factors. These factors may lead to deviated RSSI values rather the real RSSI values on Internet of things (IoT) motes. Secondly, they suggested rectifying methods to introduce corrections in an RSSI based empirical model. In support of their arguments, they also provided a comparative analysis between measurements. The multipath channel model using power delay profiles is compared for different platforms in densely equipped substation at 2.4 GHz frequency band [13]. The estimated PL model parameters differ among mote-based models and vector network analyzer (VNA) based model (For MicaZ, $\eta = 1.99$ and $L(d_0) = 63.28$ dB and for VNA, $\eta = 1.72$, $L(d_0) = 40.14$ dB where η is PL exponent and $L(d_0)$ is reference loss in dB at $d_0 = 1$ m).

Another empirical model for the smart grid is suggested in [31], which used a cellular GSM network in a suburban area. They propose to use log-distance model with slope, $\eta = 3.38$ and log-normal shadowing with standard deviation $\sigma = 9.2$ dB and a reference attenuation $L(d_0) = 65.96$ dB at 1 m. The model is claimed to be valid for 10 km radial distance. Sun-Kuk Noh and DongYou Choi [20] proposed a propagation model for LTE while considering the time and spatial characteristics. They measured the RSRP at 879 MHz using a mobile phone in downtown areas. They proposed two path loss models for indoor and outdoor environment after slight modifications in the ITU-R model [32]. One of their suggested models performed quite similar to COST231 model.

A comprehensive set of propagation models for LoRaWAN is developed by authors for urban, suburban, rural and indoor environments [22]. Here, the minimum transmitter height is 12 m. The receiver height is in the range of 2 cm to 3 m from ground. They proposed outdoor path loss models based on the log distance model. For outdoor suburban area, they suggested a base PL exponent, $\eta = 3.118$, reference path loss of 140.7 dB at 1 km and additional fading with $\sigma = 9.7$ dB standard deviation. Accordingly, a near ground receiver can further introduce an extra loss of 4.7 dB per decade. Based on ITU-R [33] and Cost231, they also proposed indoor model with multiple walls and floors penetration.

Similar to SG, many other ecosystems also require transceiver installations only few meters above the ground. Authors [34], [21], [35] presented their empirical path loss models for near ground communication in sub-GHz bands. The empirical models in [21], [35] predict the impact of foliage in suburban vegetated area and forests, respectively. Both provided data around 800 MHz. The authors of [35] also proposed the model for 450 MHz.

III. Measurement Campaigns

The prime focus of this campaign is to perform a comparative study of the link attenuation for typical SMCU deployment options at customer sites. Later, when we refer to any of these SMCU deployments, we will use the term 'TxSite' – Transmitter Site – as we presumably assign the role as transmitter node to the SMCU. DCs along pathways serve as the utility site and we presumably assign them the role as receiver node. We use the term 'RxSite' – Receiver Site – whenever we refer to any of the DC locations.

Our measurement strategy has two steps, summarized in Table II. In the first step, *Comparative Measurement Campaign*, we analyzed:

Fig. 2. Receiver locations (RxSites), red circles, in the surroundings of ET Building for Tx-Rx separation above ≈15 m, common to three installations of the transmitter (TxSites: 'basement-0', 'InHouse' and 'Outside'), a blue star.

TABLE II
MEASUREMENT CAMPAIGNS.

Campaign	Frequency	Buildings	Transmitter locations (TxSites)	Receiver locations (RxSites)	Deduced model
Comparative measurement	Four bands[a]	1 (ET)	Outdoor InHouse Basement-0	See Figs. 1(b) and 2 See Figs. 1(b) and 2 See Figs. 1(a) and 2	Outside InHouse Basement
Basement measurement	Four bands[a]	5	Basement-1 to Basement-4 and Basement-5	Not depicted	Basement

[a] 200 MHz, 434 MHz, 868 MHz, 2.4 GHz

- TxSite outside the building
- TxSite inside the same building but on ground level
- TxSite at basement of the same building representing underground indoor installation
- The RxSites (beyond 10 m up to 550 m) are unchanged for three TxSites in the campaign

The assessment of the received power of a wireless signal from an SMCU installed inside the building to the DC located on the street is very critical for planning a proper link budget in smart grids. It also becomes critical to predict excess losses realistically over these links. In Europe, multistory buildings and detached houses usually have cellars where all meters are installed. In these underground SMCU installations, the excess power loss of the SMCU-DC link is highly influenced by the building material and by the horizontal and vertical depth of SMCU inside the basement. Therefore, we extended our campaign to improve the database for the penetration losses of underground TxSites. In this second step *Basement Measurement Campaign*, we selected:

- Five additional basements, as a representation of building structures in Germany
- Each basement, from the distinct building (TxSites)
- Fewer number of RxSites outside these buildings, up to 150 m, than those in the first (*Comparative Measurement Campaign*) step

The subsequent discussion describes the overall campaign in four parts: measurement equipment, measurement procedure and measurement locations of both the campaigns.

A. Measurement Equipment

The transmitter node consisted of an R&S SMBV100B vector signal generator transmitting an unmodulated signal at 25 dBm power. The portable receiver node was an Anritsu MS2721A analyzer with a logger laptop. We used tuned antennas with feeder cables (3 m, 50 Ω). All sub-GHz antennas were tuned folded dipole antennas with a matching balun to resemble the typical size reduction of commercial antennas. We measured the horizontal gain of the sub-GHz antennas in an absorber room. The 2.4 GHz antennas were matched ground plane antennas with asymmetric feed. We calibrated these antennas in an outdoor free space environment. Measured antenna gains and feeder cable attenuations resulted in a calibrated set of received powers, which were used to normalize all losses and the antenna gains to obtain a virtual 0 dBi antenna gain. This portable setup measured the received power at various potential locations (RxSites) using only 100 Hz resolution bandwidth to reduce noise. It created a database for analysis of the overall attenuation and the small scale fading characteristics.

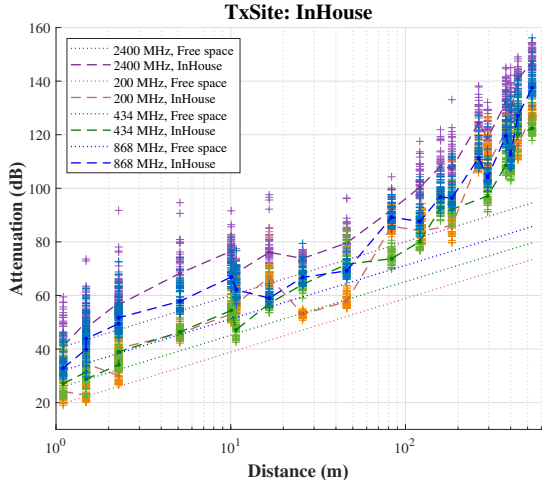

Fig. 3. Measurements for 200 MHz, 434 MHz, 868 MHz and 2.4 GHz Bands from 'InHouse' TxSite.

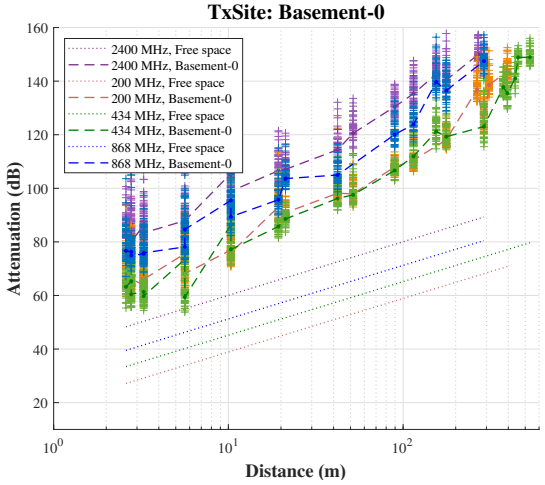

Fig. 4. Measurements for 200 MHz, 434 MHz, 868 MHz and 2.4 GHz Bands from 'basement-0' TxSite.

B. Measurement Procedure

For a total of eight TxSites (Outside, InHouse, basement-0, basement-1, basement-2, basement-3, basement-4, and basement-5) and four frequency bands (200 MHz, 434 MHz, 868 MHz, and 2.4 GHz), the complete outcome of our campaigns is obtained from thirty-two *Measurement Cycles*: A single *measurement cycle* is composed of all the *Measurements Rounds*, individually performed on each RxSite involved in this cycle.

In a *Measurement Round* on an RxSite within a certain measurement cycle, the signal analyzer measured the power of the received signal in a semi-automated procedure. In order to determine the mean attenuation and to level out small-scale fading characteristics, this procedure sensed 50 power samples at this RxSite within fifteen minutes. These samples were collected consecutively on a manually placed grid pattern, in a plane perpendicular to the link direction, bounded in square meters. Linear averaging of the calibrated received power at this RxSite in relation to the transmitted power gave the attenuation.

C. Locations of the Comparative Measurement Campaign

All measurements were performed in the city of Dortmund, providing a typical combination of urban and suburban housing. The three TxSites represent distinct placements of the transmitter in the ET building (Faculty of Electrical and Information Technology) at the campus of TU Dortmund. In our subsequent discussions, *'basement-0'*, *'InHouse'* and *'Outside'* terminologies will uniquely refer to certain TxSite, with the following characteristics:

1) 'basement-0': On the first TxSite, the transmitter's location is inside a sanitation room, near its outer wall. The room is located at the subterranean basement floor of the ET building. This windowless room has walls and ceilings of reinforced concrete and a closed steel door. The antenna's position is at 1.5 m floor height but was about 2 m below ground. The nearest RxSite was at ground floor, vertically nearly above but outside the building. This RxSite is 'A' in Fig. 1(a).

TABLE III
BASEMENT SPECIFICATIONS.

TxSite	Building type	Tx depth	Windows/doors
Basement-0	Multistory ET building	20 cm inside/ Floor -1	No window/ a metal door
Basement-1	A detached house	6 m inside/ Floor -1	Ventilation window/ a door
Basement-2	Multistory building	20 cm inside/ Floor -1	Ventilation window/ a wooden door
Basement-3	A detached house	2 m inside/ Floor -1	Window on ground floor/ No
Basement-4	Highrise building	11 m inside/ Floor -2	No window/ metal door
Basement-5	A detached house	2 m inside/ Floor -1	Ventilation window/ a wooden door

2) 'InHouse': The second TxSite is inside a room with office characteristic at ground floor. The antenna was in a corner with the outer wall, 20 cm away from the sidewalls at 150 cm height. The first RxSite was outside the building at the same height, just opposite to the transmitter. This RxSite is shown in Fig. 1(b) as 'A'.
3) 'Outside': The very same point 'A' shown in Fig. 1b is now the third TxSite. It is outside the building 20 cm away from the wall and at 150 cm height. Here, the first RxSite was 'B' beside 'A' and at the same height of transmitter.

Fig. 1 contains RxSites with link distances up to 10 m where Fig. 1(a) shows RxSites for the 'basement-0' TxSite and Fig. 1(b) shows RxSites common to both 'InHouse' and 'Outside' TxSites. Fig. 2 depicts RxSites with link distances above 10 m up to 500 m. These RxSites (beyond 10 m) are common to 'basement-0', 'InHouse' and 'Outside' TxSite. In any map, RxSites are shown in red circles while the TxSite, if given, is marked with a blue star (all maps are captured in Google Earth).

This campaign consisted on twelve *measurement cycles*. These cycles were all combinations between TxSites and the

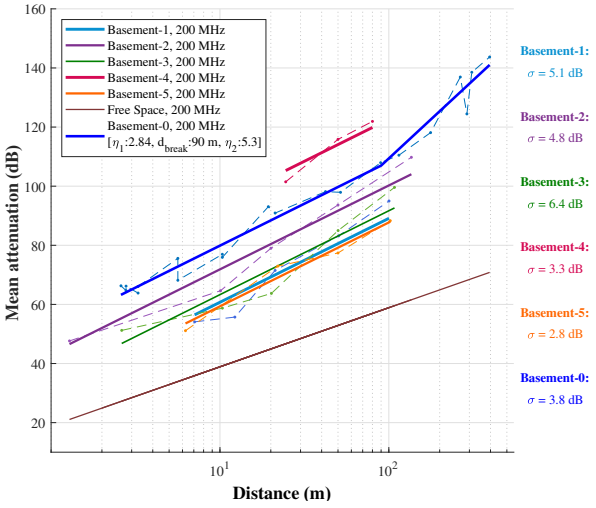

Fig. 5. Attenuation in basement communication for 200 MHz (dotted lines connect the observed mean attenuations on RxSites for the respective basement).

frequency bands (Outside, InHouse, basement-0) x (200 MHz, 434 MHz, 868 MHz and 2.4 GHz). Each *measurement cycle* for 'basement-0' involved all RxSites shown in Figs. 1(a) and 2. Each *measurement cycle* for 'InHouse' and 'Outside' involved all RxSites shown in Figs. 1(b) and 2.

D. Locations of the Basement Measurement Campaign

In the *Basement Measurement Campaign*, we performed measurements at five residential buildings in the suburban area of Dortmund.

The TxSites 'basement-1', 'basement-3', and 'basement-5' are the part of distinct independent detached houses. 'basement-2' is the part of a multi-story residential apartment building. 'basement-4' belongs to a 22-floors apartment building. We decided to install our transmitter approximately close to energy meters in these buildings. In a detached house, usually energy meters are installed in an alley/corridor at the basement floor. However, multi-story buildings usually have a dedicated room in the basement for all energy meters. The location maps with TxSite and respective RxSites for 'basement-1' to 'basement-5' are not present in this document due to the limitation of space. Construction materials of these buildings include clay bricks, natural stone and reinforced concrete with construction between 1900 and 2000. Table III gives necessary details of these basements.

The next section gives an overview of the data analysis and subsequently, our proposed channel model. All these results are normalized to 0 dBi antenna gain and give the average attenuation at each RxSite. Averaging the power fluctuations at each RxSite is needed due to the 'fast fading' mechanism caused by the rich scattering environment.

IV. Key Results of the Measurement Campaign

A. Analysis of the Comparative Campaign

The measurements from two out of three TxSites, in the comparative campaign, are presented in Figs. 3 and 4. As expected, the plots for the 'Outside' TxSite show an average of 35, 34, 42, and 40 dB lower propagation losses on its RxSite at 200, 434, 868, and 2400 MHz band respectively as compared to respective RxSite in its counterpart, the 'basement-0' TxSite (at ET building). 'basement-0' TxSite introduced the higher propagation losses due to the underground placement of the transmitter node. However, the 'InHouse' TxSite plots remained in the middle of other two TxSites. The propagation loss trend over frequency bands is also visible. Higher frequencies such as 2.4 GHz and 868 MHz presented more mean attenuation on its RxSites as compared to the lower frequencies. Although 200 MHz and 434 MHz losses are very close to each other, an interesting phenomenon is apparent for these bands in 'InHouse' and 'basement-0' TxSites. With 'InHouse' TxSite, 200 MHz performed better (up to 14 dB less than that of 434 MHz) on its RxSites, especially at shorter distances (up to 10 m). On the other hand, 434 MHz performed better (2 to 8 dB less than that of 200 MHz) with 'basement-0' TxSite, on most of the RxSites at lower distances (up to 100 m). Since all measurements of a certain TxSite were done on exactly the same RxSites, there is no obvious reason for this phenomenon. Probably the size of the steel mesh inside the concrete may shield excessively at longer wavelengths.

B. Analysis of the Basement Measurement Campaign

In this part of the campaign, the observed distance dependent attenuations are very similar to 'basement-0' of the comparative campaign: Fig. 5 shows one of these plots. However, the overall impact of outer walls on the signal penetration differs between buildings as well as between frequencies. Signal penetration at various frequencies is not just a scalar multiple of the factor to which these frequencies relate to each other; rather we observed that some frequencies penetrated better than the others did. These differences may depend on the construction structure, which behaves differently for different frequencies and geometries. In all frequency bands, estimated plots of 'basement-4' – a high-rise building – always produced highest while 'basement-5' always produced least attenuated signals.

From the remaining three basements, the estimated path loss of 'basement-3' always stays in the middle of 'basement-1' and 'basement-2'. Additionally, 'basement-1' produced the lowest attenuation at 200 MHz and 434 MHz and the highest attenuation at 868 MHz and 2.4 GHz.

C. Breakpoint Analysis

Even outside buildings, the distance dependent attenuation is higher than the predicted free space propagation losses. The path loss exponent exceeds the nominal free space value of 2 at larger distances. One main reason is that as we move away from the transmitter, surrounding buildings and other structures obstruct the line of sight. In most cases, no exact knowledge is available for the respective geometry and the materials inside and outside the target and the surrounding buildings. Even if we would have such an information, a complex Ray tracing model considering diffraction, reflection and scattering is not desirable: This is due to its complex

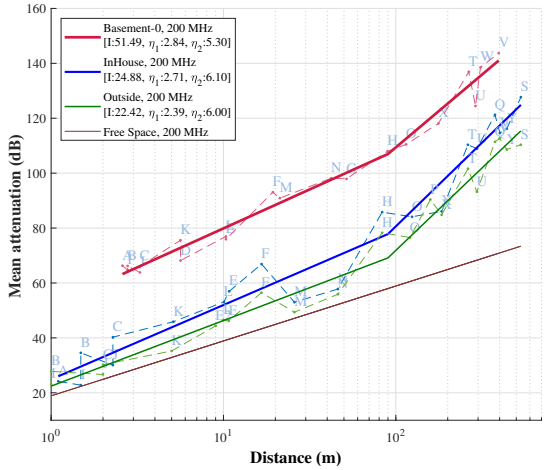

Fig. 6. Two-slope linear estimations for 200 MHz with breakpoint distance d_{break}, at 90 m (dotted lines connect the observed mean attenuations on the RxSites. Here, letters denote RxSites from Figs. 1 and 2).

TABLE IV
SINGLE SLOPE ESTIMATIONS.

TxSite	Band (MHz)	L_R (dB)	10η –	RMSE (dB)	R^2 –
Outside	200	16.14	32.96	7.19	0.95
	434	14.66	33.29	8.67	0.92
	868	22.57	33.2	8.61	0.92
	2400	31.18	32.99	8.95	0.92

* L_R is reference loss at 1 m

TABLE V
BREAKPOINT ESTIMATIONS (868 MHZ).

d_{break}	50	60	70	80	90	100	110	120
L_R	39.8	39.8	39.8	39.8	38.4	38.4	38.4	38.4
η_1	1.98	1.98	1.98	1.98	2.26	2.26	2.26	2.26
η_2	5.1	5.5	5.8	6.2	5.9	6.2	6.5	6.9
RMSE	5.32	5.21	5.18	5.24	5.23	5.12	5.04	5.02

* L_R is reference loss at 1 m and d_{break} is given in meters

computing efforts and the instable results if the arrangement of objects in the environment changes. Here, we concentrate on an abstract model that reflects the excess attenuation by a multi-slope path loss exponent. The basic modelling approach assumes that the slope changes at a certain reference distance, typically at 1 m. However, our measurements in Figs. 3 and 4 clearly show that proper modelling with least error on estimation needs another breakpoint to split the path loss exponent at a distance of about 100 m.

V. PROPOSED MODEL

Summarizing the measurements, we introduce the following:

- A single constant A_p, models all penetration losses at the reference distance d_{ref}. The value of this constant depends on the frequency and the type of the building. It also includes other losses such as polarization losses. We chose $d_{ref} = 1$ m. This has the advantage that A_p can be seen as an estimation for the penetration loss with respect to the free space model at reasonable small distances up to 10 m
- Starting with d_{ref}, we incorporate the first path loss exponent, η_1 until breakpoint distance
- At the breakpoint distance d_{break}, the final slope starts with a path loss exponent, η_2
- For deep indoor location, there is no line of sight. A superseded small scale fading A_{SSF}, will be Rayleigh fading and might be considered to cause an additional attenuation i.e., $A_{SSF} = A_{\text{rayleigh}}$
- For outdoor locations, either with a line of sight or with an extraordinary reflection path, the superseded small scale fading will tend to be Ricean fading. Therefore, $A_{SSF} = A_{Ricean}$ might be selected with an appropriate Ricean factor. The penetration loss A_p, is then set to zero

Finally, our model uses the following equation for the path loss P_L, given in dB:

$$P_L(d \leq d_{\text{break}}) = 32.44 + A_p + A_{SSF} + 10\eta_1 log_{10}(d/1m), \quad (1)$$

$$P_L(d > d_{\text{break}}) = P_L(d_{\text{break}}) + 10\eta_2 log_{10}(d/d_{\text{break}}), \quad (2)$$

where *'d'* is the separation distance in meters between SMCU and DC.

When introducing directional high gain antennas into the proposed model, the user should consider these two facts:

1) In most cases, there will be no line of sight link. Due to reflections and rich scattering, the antenna's directional pattern is less beneficial or may even expose negative gain
2) Antennas without or with unspecified gain may even suffer from negative gain due to a) antenna misalignment, b) ohmic losses, c) imperfect antenna matching or d) detuning of the antenna by objects in the direct vicinity of the antenna itself

A. Parameter Estimation

Simple linear estimations are not suitable due to its low quality of fit to measured data as depicted by the coefficients of determination R^2, in Table IV ('Outside' TxSite is given only). Therefore, one of the tasks is to identify d_{break} and both path loss exponents for the model in (1) and (2). We used simple regression method of least squares to minimize error in the estimation. A_p however, takes into account the individual factors depending on the building. The optimum value of d_{break} is estimated by comparing the root mean square error (RMSE) of two-slope models on various breakpoints such as 50, 60, 70, 80, 90, 100, 110, and 120 m. As an example, Table V provides these estimations for 868 MHz ('InHouse' TxSite). The breakpoint for all bands has a nearly flat optimum value therefore $d_{\text{break}} = 90$ m is selected for all frequency bands. In an ideal world, A_p of all 'Outside' measurements could ideally be 0 dB, however our measurements deviate from it by the small range of only -2.2 to 3.2 dB. Fig. 6 shows one

TABLE VI
MODEL PARAMETERS.

Band (MHz)	TxSite	A_p (dB)	η_1 –	η_2[a] –	σ (dB)	RMSE (dB)	R^2 –
200	Outside	0	2.39	6	4.79	4.67	0.98
	InHouse	6	2.71	6.1	6.29	6.14	0.97
	Basement	11–32	2.84	5.3	3.75	3.67	0.98
434	Outside	0	2.14	6.9	5.27	5.15	0.97
	InHouse	1	2.57	5.4	3.42	3.34	0.99
	Basement	8–22	3	5.1	4.31	4.22	0.98
868	Outside	0	2.27	6.6	4.29	3.08	0.98
	InHouse	7	2.26	5.9	5.34	5.23	0.97
	Basement	13–31	2.85	6.4	3.17	3.08	0.98
2400	Outside	0	2.02	7.1	4.94	4.83	0.98
	InHouse	6	2.3	6.6	4.08	3.99	0.98
	Basement	13–33	2.94	4.5	2.98	2.91	0.98

[a] Second path loss exponent η_2, is considered after the breakpoint distance d_{break}, at 90 m

of these two-slope estimation plots. In our "Outside" models, the path loss exponents, split at breakpoint, differ by 3.61 at 200 MHz and by 4.76 in 434 MHz which is close to 4.95 at 500 MHz [36]. To propose the single "Basement" model for all the basements, we took the well-conditioned η_1 value for a certain band from 'basement-0' estimations, as given in Table VI, and used it to predict linear propagation losses for that band in other basements ('basement-1' to 'basement-5'). Fig. 5 shows this linear estimation at one of the frequency bands (i.e. 200 MHz). These estimations suggest the range for A_p as given in Table VI. In our whole campaign, standard deviation of the differences between the estimated and measured attenuation in a certain frequency band ranges from 1 dB to 9 dB. Fig. 5 shows standard deviation σ, for 'basement-0' to 'basement-5' estimations at 200 MHz and Table VI gives σ, RMSE and R^2 of the estimations at each frequency band for the proposed model of "Outside", "InHouse" and "Basement" installations.

B. Path Loss Model with Parameters

The path loss exponents do not show noticeable dependence on the carrier frequency. Therefore, Table VI presents all the model parameters without any additional formulation. Our measurements give consistent path losses up to 500 m. Therefore, we believe our model is valid within this range using these sets of parameters. A heuristic selection of A_p within the specified range after assessment of the building structures and the indoor location is suitable for link budget planning. For modeling a random situation in simulations, one can assume A_p as a uniformly distributed random variable over the specified range. For worst-case link budget planning, the maximum value of A_p must be selected. We also suggest that A_p of basement-4 (high-rise building, transmitter two floors below ground) should not be included in planning considerations. We discourage deep underground wireless communication (for I2O and O2I) to optimally utilize precious frequency resources. A cable connection on the local hop towards an external antenna/gateway device outside the exterior wall of the building or a wireless repeater may be installed instead.

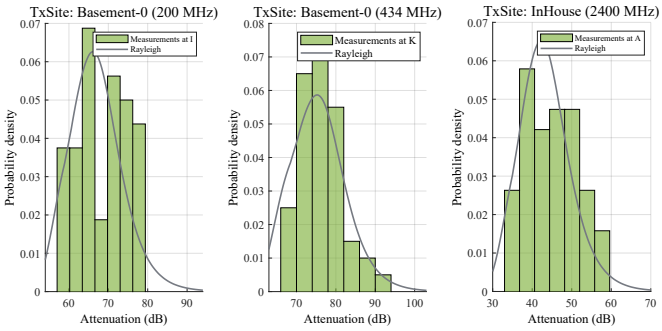

Fig. 7. Distribution of measurements on selected RxSites.

Fig. 7 gives exemplary measurements of selected RxSites from our campaign, which indicate that these observations correspond to a Rayleigh distribution. In simulations, one can derive A_{rayleigh} calculated by $A_{\text{rayleigh}} = 10\ log_{10}\ (R_F)$, where R_F is a squared Rayleigh random number with proper scaling so that R_F itself has a variance of 1. For link budget planning, we suggest to take the value of R_F from the cumulative density function of R_F at a given outage probability. Similar considerations hold for outdoor deployment, however, with Ricean fading.

C. Comparison with Standard Propagation Models

We will compare our findings with relevant propagation models from the literature. None of these models explicitly refers to a subterranean reception.

IEEE P802.11 TGah [37] gives only a penetration loss of 10 dB for indoor reception and a floor attenuation factor without referring to a specific frequency. Winner-II [38] provides a large set of scenarios. These scenarios were compiled from a meta study based on a certain set of publications. Only three of these scenarios (A2, B4, and C3) model indoor to outdoor communication. Due to its heterogeneous input data, Winner-II gives different values for the penetration loss for different scenarios. In addition, it is only applicable for the frequencies above 2 GHz. Moreover, Winner-II concentrates on the correct modelling of small scale fading and multipath characteristics but not on the path loss. The Winner-II O2I basement entry loss ranges from 20 dB to 50 dB at 5 GHz, which is nearly 1.5 times the range we observed for 2.4 GHz ("Basement" model in Table VI). Table VII provides various BEL measurements from the literature.

The ITU-R P.1238-10 [39] also has large emphasis on the multipath characteristics but covers the frequency range from 300 MHz to about 73 GHz. However, this model has been set up primarily for indoor communication. It lacks numbers for penetration losses and does not provide any mean to calculate the excess loss caused by underground reception. ITU-R P.1411-10 [40] also concentrates on the multipath characteristics but primarily for outdoor scenarios. Table VIII summarizes the relevant standards.

ITU-R P.2040-1 [41] gives detailed information to calculate penetration losses from the material constants of typical building structures with various geometries. Nevertheless, there is

TABLE VII
BUILDING ENTRY LOSSES.

Ref.	Frequency (MHz)	Build entry loss (dB)
[23]	169, 434 and 868	33.7, 31.8 and 39.6, respectively
[26]	169	7.5 (σ=4.5)
[27]	1500 and 3000	61 and 71, respectively
[28]	3000	11 – 27
[24]	820.5	13 dB more at floor level -1 than 0
[38]	5000	20 – 50 (in basement), 10 – 30 (at floor level 0)
[37]	900 or else	10
[43]	1500 and 3000	58 and 68, respectively (in basement)
	3000	18 – 29
	220	9.1 – 14 .8 (σ=3.5)
	588	7 – 17.8 (σ=3.5)
	756	8.5 – 16 (σ=5.5)
[42]	1000 and 2000	39 and 35, respectively

TABLE VIII
STANDARD PROPAGATION MODELS.

Ref.	Standard description	Model environments
[39]	ITU-R P.1238 provides multipath indoor models with multi-floor penetrations. However, it does not consider basement entry losses.	Residential, Office, Commercial Factory, Corridor [Indoor]
[37]	IEEE P802.11 models path loss for IEEE802.11 sub-1GHz operation gives building and floor attenuations irrespective of any frequency.	Macro deployment, Pico/Hotzone [outdoor]; and Indoor models
[38]	The relevant Winner-II scenarios (A2, B4 and C4) models path loss only above 2 GHz.	Campus Area [O2I]
[40]	ITU-R P.1411 provides multipath models for outdoor communication.	Urban and Suburban [Outdoor]
[43]	Out of many campaigns for BEL measurements in ITU-R P.2346, only one campaign measured basement entry losses.	Huge set of various environments
[41]	It only provides guidance on electrical characteristics of building materials without any direct connection to any of the path loss models.	

no direct connection to P.1238-10 [39] nor to P.1411-10 [40]. There is an extension ITU-R P.2109-1 [42] that explicitly covers the loss of exterior walls. Even then, P.1238-10 and P.1411-10 do not provide a simple method to estimate typical path losses for underground reception.

ITU-R P2346-3 [43] is a compilation of measurements for building entry loss from a large number of different publications. Therefore, it lacks consistency in its findings. Only one of its measurements reported penetration losses into a basement (parking lot). However, these measurements were performed only at 1.5 and 3 GHz. Moreover, the authors of this part derived the entry loss without any connection to the attenuation caused by the link distance. Finally, they concluded that the penetration loss into a basement could be about 30 dB higher than that predicted by ITU-R P.2109-1 [42]. This supports our findings that the penetration loss is a major part of the link attenuation in case of deep indoor communication. Moreover, the penetration losses reported in ITU-R P.2346-3 match with the large variation of the penetration losses that we identified. Besides the penetration loss, our work presents a simple model that includes the dependency on the link distance and is derived from consistent measurements from 200 MHz up to 2.4 GHz.

VI. CONCLUSION

Smart grid, a visionary approach to utilize green energy in a very efficient way, has been facing strong challenges not only in its primary (power) domain but also in the communication domain. The wireless technologies such as 802.11ah, 802.11n, LoRaWAN and LTE (unlicensed variant) which can operate in unlicensed bands have a potential to establish NAN with existing grid infrastructure and indoor SMCU installations. However, the accurate link budgeting is essential. Therefore, we have proposed an empirical model for optimum link budgeting on genuine observations over low distance range and low transceiver heights in SMCU-DC wireless links. The proposed model is applicable for the three sub-GHz bands (868 MHz, 434 MHz, and 200 MHz) and for the 2.4 GHz band.

SMCUs were installed in three different options for path loss measurements. Firstly, the SMCU (the transmitter node) was installed outside the building; secondly, installed on the exterior wall of the ground floor inside the building and finally, the critical one, where SMCUs were installed in basements. The measurement results clearly show that single slope estimations do not predict the path losses accurately in suburban environments. A realistic estimation requires a linear two-slope model with 90 m breakpoint distance, which increases the quality of fit up to 6.3% as compared to single slope estimation. Results show that in the "Outside" case, lowest and highest first path loss exponents η_1 are observed in 2.4 GHz and 200 MHz bands, which are 2.02 and 2.4, respectively. Similarly, extremes of the second path loss exponent η_2 are 6.0 and 7.1 in 200 MHz and 2.4 GHz bands, respectively. In the "InHouse" installations, η_1 extremes are 2.3 and 2.7 in 200 MHz and 868 MHz, respectively. Similarly, η_2 extremes are 5.4 and 6.6 in 434 MHz and 2400 MHz, respectively. In "Basement" installations, η_1 extremes are 2.8 and 3.0 in 200 MHz and 434 MHz, respectively. Similarly, η_2 extremes are 4.5 and 6.4 in 2400 MHz and 868 MHz, respectively. The comparatively lower additional power penalty of 8 dB to 22 dB is imposed by the 434 MHz band for deep-indoor communication, while other bands bring penalties higher than 434 MHz but similar to each other.

The 22 floor high-rise building offered the highest additional power requirements for outdoor-to-deep-indoor communication, which ranges from 35.8 to 46.7 dB. In this building, the basement was two floors below ground level. Therefore, we deliberately ignored these measurements in our final model. We suggest inexpensive alternatives such as wired links and/or a repeater between indoor meter and outdoor antenna rather than increasing the precious link budget and/or putting huge capital at stake in purchasing expensive licensed bands for long range cellular network for distribution management in future VPP and DER prevalent smart grids.

REFERENCES

[1] L. Ferreira, M. Kuipers, C. Rodrigues, and L. M. Correia, "Characterisation of signal penetration into buildings for GSM and UMTS," in *Proc. IEEE ISWCS*, Sep. 2006.

[2] F. N. N. Roadmap, "From network to system; 2017 – 2021 network development timetable," Berlin, Germany, 2017. [Online]. Available: https://www.vde.com/en/fnn/topics/fnn-roadmap

[3] European Union, "Communication from the commission to the European parliament - A clean planet for all - A European strategic long-term vision for a prosperous, modern, competitive and climate neutral economy," 2018, COM(2018) 773 final. [Online]. Available: https://ec.europa.eu/clima/eu-action/climate-strategies-targets/2050-long-term-strategy_en

[4] M. Stötzer, I. Hauer, M. Richter, and Z. A. Styczynski, "Potential of demand side integration to maximize use of renewable energy sources in Germany," *Appli. Energy*, vol. 146, pp. 344–352, May 2015.

[5] B. Kroposki, B. Johnson, Y. Zhang, V. Gevorgian, P. Denholm, B. Hodge, and B. Hannegan, "Achieving a 100% renewable grid: Operating electric power systems with extremely high levels of variable renewable energy," *IEEE Power Energy Mag.*, vol. 15, no. 2, pp. 61–73, Mar. 2017.

[6] A. Kulmala, M. Alonso, S. Repo, H. Amaris, A. Moreno, J. Mehmedalic, and Z. Al-Jassim, "Hierarchical and distributed control concept for distribution network congestion management," *IET Generation, Transmiss. Distribution*, vol. 11, no. 3, pp. 665–675, Feb. 2017.

[7] M. Pasetti, S. Rinaldi, and D. Manerba, "A virtual power plant architecture for the demand-side management of smart prosumers," *Appl. Sci.*, vol. 8, no. 3, 2018.

[8] F. Heimgaertner and M. Menth, "Distributed controller communication in virtual power plants using smart meter gateways," in *Proc. IEEE ICE/ITMC*, Jun. 2018, pp. 1–6.

[9] L. Mariam, M. Basu, and M. F. Conlon, "Microgrid: Architecture, policy and future trends," *Renewable Sustainable Energy Reviews*, vol. 64, pp. 477–489, Oct. 2016.

[10] J. A. Cortés *et al.*, "Feasibility study of power line communications for backhauling outdoor small cells," *IEEE Access*, vol. 9, pp. 30 135–30 153, 2021.

[11] H. Früh, "Field-test based comparison of LTE and PLC communication technologies for smart grid applications," *Proc. IEEE CIRED*, Jan. 2020.

[12] L. d. M. B. A. Dib, V. Fernandes, M. de L. Filomeno, and M. V. Ribeiro, "Hybrid PLC/wireless communication for smart grids and internet of things applications," *IEEE Internet Things J.*, vol. 5, no. 2, pp. 655–667, 2018.

[13] R. M. Sandoval, A.-J. Garcia-Sanchez, J.-M. Molina-Garcia-Pardo, F. Garcia-Sanchez, and J. Garcia-Haro, "Radio-channel characterization of smart grid substations in the 2.4-GHz ISM band," *IEEE Tran. Wireless Commun.*, vol. 16, no. 2, pp. 1294–1307, 2017.

[14] R. M. Sandoval, A. Garcia-Sanchez, and J. Garcia-Haro, "Improving RSSI-based path-loss models accuracy for critical infrastructures: A smart grid substation case-study," *IEEE Trans. Ind. Inform.*, vol. 14, no. 5, pp. 2230–2240, May 2018.

[15] V. S. Abhayawardhana, I. J. Wassell, D. Crosby, M. P. Sellars, and M. G. Brown, "Comparison of empirical propagation path loss models for fixed wireless access systems," in *Proc. IEEE VTC-spring*, May 2005.

[16] T. K. Sarkar, Zhong Ji, Kyungjung Kim, A. Medouri, and M. Salazar-Palma, "A survey of various propagation models for mobile communication," *IEEE Antennas Propag. Mag.*, vol. 45, no. 3, pp. 51–82, Jun. 2003.

[17] C. Phillips, D. Sicker, and D. Grunwald, "Bounding the practical error of path loss models," *International J. Antennas Propag.*, vol. 2012, pp. 1–12, Jun. 2012.

[18] S. Rauh, J. Robert, T. Lauterbach, G. Kilian, H. Lieske, and A. Heuberger, "Long-term LPWAN sub-GHz deep indoor-to-outdoor channel model," in *Proc. IEEE VTC-fall*, Sep. 2019.

[19] M. Kacou, V. Guillet, G. El Zein, and G. Zaharia, "A multi-wall and multi-frequency home environment path loss characterization and modeling," in *Proc. EUCAP*, Apr. 2018.

[20] C. Sun-Kuk, Noh; DongYou, "Propagation model in indoor and outdoor for the LTE communications," *Int. J. Antennas Propag.*, p. 6, 2019.

[21] J. C. Silva, G. L. Siqueira, and P. V. G. Castellanos, "Propagation model for path loss through vegetated environments at 700 – 800 MHz band," *J. Microwaves Optoelectronics Electromagn. Applicat.*, vol. 17, pp. 179–187, Mar. 2018.

[22] R. El Chall, S. Lahoud, and M. El Helou, "LoRaWAN network: Radio propagation models and performance evaluation in various environments in lebanon," *IEEE Internet Things J.*, vol. 6, no. 2, pp. 2366–2378, Apr. 2019.

[23] H. Lieske, T. Lauterbach, J. Robert, G. Kilian, and A. Heuberger, "Indoor-to-outdoor radio channel measurements in sub-GHz unlicensed frequency bands," in *Proc. IEEE Smart SysTech*, Jul., 2015, pp. 1–9.

[24] K. M. Malarski, J. Thrane, M. G. Bech, K. Macheta, H. L. Christiansen, M. N. Petersen, and S. Ruepp, "Investigation of deep indoor NB-IoT propagation attenuation," in *Proc. IEEE VTC-fall*, Sep. 2019.

[25] ETSI TR 138 901 V14.3.0 (2018-01), "Study on channel model for frequencies from 0.5 to 100 GHz," ETSI, 3GPP, Tech. Rep., Jan. 2018.

[26] F. Fuschini, M. Barbiroli, G. E. Corazza, V. Degli-Esposti, and G. Falciasecca, "Analysis of outdoor-to-indoor propagation at 169 MHz for smart metering applications," *IEEE Trans. Antennas Propag.*, vol. 63, no. 4, pp. 1811–1821, 2015.

[27] D.-W. Kim, J.-B. Jin, and S.-S. Oh, "Empirical analysis of building entry loss from outside of office building with large lobby into a basement at 1.5 and 3 GHz," *IEEE Antennas Wireless Propag. Lett.*, p. 1, 2021.

[28] S. Salous *et al.,* "Chapter 3 - IRACON channel measurements and models," in *Inclusive Radio Commun. for 5G and Beyond*, C. Oestges and F. Quitin, Eds. Academic Press, 2021, pp. 49–105.

[29] W. Xu *et al.*, "Measurement, characterization and modeling of LoRa technology in multi-floor buildings," *IEEE Internet Things J.*, p. 1, 2019.

[30] B. Holfeld, S. Jaeckel, L. Thiele, T. Wirth, and K. Scheppelmann, "Smart grid communications: LTE outdoor field trials at 450 MHz," in *Proc. IEEE VTC-spring*, May 2015.

[31] O. N. Anthony and O. O. R, "Empirical model of cellular signal propagation loss for smart grid environment," *Int. J. Smart Grid Clean Energy*, vol. 5, no. 4, pp. 272–279, 2016.

[32] Recommendation ITU-R P.1411-5 (10/2009), "Propagation data and prediction methods for the planning of short-range outdoor radiocommunication systems and radio local area networks in the frequency range 300 MHz to 100 GHz," ITU-R, Tech. Rep., 2009.

[33] Recommendation ITU-R P.1238-3 (04/2003), "Propagation data and prediction methods for the planning of indoor radiocommunication systems and radio local area networks in the frequency range 900 MHz to 100 GHz," ITU-R, Tech. Rep., 2003.

[34] H. Klaina, A. Vazquez Alejos, O. Aghzout, and F. Falcone, "Narrowband characterization of near-ground radio channel for wireless sensors networks at 5G-IoT bands," *Sensors*, vol. 18, no. 8, 2018.

[35] Y. S. Meng, Y. H. Lee, and B. C. Ng, "Empirical near ground path loss modeling in a forest at VHF and UHF bands," *IEEE Trans. Antennas Propag.*, vol. 57, no. 5, pp. 1461–1468, May 2009.

[36] J. Huang *et al.*, "Channel measurements and modeling for 400–600-MHz bands in urban and suburban scenarios," *IEEE Internet Things J.*, vol. 8, no. 7, pp. 5531–5543, Apr. 2021.

[37] R. Porat, S. Yong, and K. Doppler, "IEEE P802.11 Wireless LANs: TGah Channel Model – Proposed Text Rev. 4," IEEE, Tech. Rep., Mar. 2015.

[38] IST-4-027756 WINNER II, "WINNER II Channel Models - Deliverable 1.1.2, Part I and II," Sep. 2007.

[39] Recommendation ITU-R P.1238-10 (08/2019), "Propagation data and prediction methods for the planning of indoor radiocommunication systems and radio local area networks in the frequency range 300 MHz to 450 GHz," ITU-R, Tech. Rep., 2019.

[40] Recommendation ITU-R P.1411-10 (08/2019), "Propagation data and prediction methods for the planning of short-range outdoor radiocommunication systems and radio local area networks in the frequency range 300 MHz to 100 GHz," ITU-R, Tech. Rep., 2019.

[41] Recommendation ITU-R P.2040-1 (07/2015), "Effects of building materials and structures on radiowave propagation above about 100 MHz - P Series - Radiowave propagation," ITU-R, Tech. Rep., 2015.

[42] Recommendation ITU-R P.2109-1 (08/2019), "Prediction of building entry loss," ITU-R, Tech. Rep., 2019.

[43] Report ITU-R P.2346-3 (05/2019), "Compilation of measurement data relating to building entry loss," ITU-R, Tech. Rep., 2019.

Muhammad Babar Ali received his master's degree from University of Engineering and Technology, Lahore, Pakistan in 2012. He received bachelor's degree in Computer Engineering from COMSATS University, Lahore, Pakistan in 2006. Currently, he is pursuing for his Ph.D. degree at Communication Technology Institute, TU Dortmund University, Dortmund, Germany.

He worked as Lecturer at Electrical Engineering Department, COMSATS University Lahore until 2014 and then as Assistant Professor until 2017. His research interests include Low Power Wide Area Networks and communication in Smart Grid Neighbourhood Area Networks.

Wolfgang Endemann (M'15) received the Diploma and the Ph.D. degree in Electrical Engineering from TU Dortmund University, Dortmund, Germany, in 1990 and 1998, respectively.

After receiving his Diploma, he joined the Communication Technology Institute at TU Dortmund, where he worked on motion vector-based video processing and image coding. After receiving the doctoral level in 1998, his research topics include signal processing, modeling of wireless channels, wireless network technologies, and their hardware implementation aspects.

Rüdiger Kays (M'03–SM'13) received the Diploma and the Ph.D. degree in Electrical Engineering from TU Dortmund University, Dortmund, Germany, in 1981 and 1986, respectively.

He was with the Grundig AG, Nuremberg, Germany, where he was responsible for the company's research and advanced development department. Since 1999, he has been a Professor in Communications Technology at TU Dortmund University. His research interests include wireless local networks, car-to-car communication and signal processing, and transmission for electronic media applications.